Rotaxane or Pseudorotaxane? That Is the Question![†]

Peter R. Ashton,[‡] Ian Baxter,[§] Matthew C. T. Fyfe,[‡] Françisco M. Raymo,[‡] Neil Spencer,[‡] J. Fraser Stoddart,*[,‡] Andrew J. P. White,[§] and David J. Williams[§]

Contribution from The School of Chemistry, The University of Birmingham, Edgbaston, Birmingham B15 2TT, UK, and The Chemical Crystallography Laboratory, Department of Chemistry, Imperial College, South Kensington, London SW7 2AY, UK

Received September 5, 1997

Abstract: A series of secondary dialkylammonium ions $(RCH_2)_2NH_2^+$ have been prepared, and their binding properties toward the macrocyclic polyether dibenzo[24]crown-8 (DB24C8) evaluated. By using this information, a route to a kinetically stable rotaxane-like entity—stabilized by noncovalent bonding interactions between the DB24C8 macroring and the ammonium center—was established, in which the crown ether slips over a dialkylammonium ion's stopper groups (R). However, we have found that the kinetic stability of this rotaxane-like entity is extremely dependent on the nature of the solvent in which it is dissolved, suggesting that pseudorotaxanes lie in the fuzzy domain between two sets of extremes, wherein a beadlike macrocycle and a dumbbell-like component may either (1) exist as a rotaxane or (2) be completely disassociated from one another.

Introduction

The quest for nanoscopic device-like systems, based upon molecular components,[1] has led to the rapid growth of a new field of chemical synthesis involving the production of interlocked molecules[2] such as rotaxanes.[3,4] In these molecular assemblies,[5] a beadlike component (i.e., a macrocycle) is bound mechanically to a dumbbell-like species so that the activation energy for "dumbbell"-extrusion is too high to be overcome at ambient temperature. During the past 5 years, we have developed a novel synthetic strategy—namely, *slippage*[6,7]—for the construction of rotaxane-like assemblies (Figure 1) that relies upon (1) the size complementarity between the macrocycle and the "dumbbell's" stoppers, in addition to (2) stabilizing noncovalent bonding interactions between the macrocycle and the "dumbbell's" rod. In this strategy, the macrocycle **M** and the "dumbbell" **D** are synthesized separately, before being heated together in solution so that the free energy of activation (i.e., $\Delta G^{\ddagger}_{on}$) for the slippage of **M** over **D**'s stoppers can be overcome. The noncovalent bonding interactions present in the rotaxane-like structure **R** make it more stable than its precursors, viz., **M** and **D**, by $\Delta G°$—i.e., the free energy of complexation—so that the free energy of activation for its dissociation (i.e., $\Delta G^{\ddagger}_{off}$) becomes insurmountable when the solution is cooled to ambient temperature. To date,[6] we have utilized the supramolecular assistance to synthesis[8] provided by, inter alia, aryl−aryl stacking interactions between π-electron deficient bipyridinium-based "dumbbells" (or macrocycles) and π-electron rich

* To whom correspondence should be addressed. Current address: Department of Chemistry and Biochemistry, University of California, Los Angeles, 405 Hilgard Avenue, Los Angeles, CA 90095.

[†] Molecular Meccano, Part 33. For Part 32, see: Amabilino, D. B.; Ashton, P. R.; Stoddart, J. F.; White, A. J. P.; Williams, D. J. *Chem. Eur. J.* In press.

[‡] University of Birmingham.

[§] Imperial College.

(1) (a) de Silva, A. P.; McCoy, C. P. *Chem. Ind. (London)* **1994**, 992−996. (b) Drexler, K. E. *Annu. Rev. Biophys. Biomol. Struct.* **1994**, *23*, 377−405. (c) Whitesides, G. M. *Sci. Am.* **1995**, *273* (3), 114−117. (d) Ashton, P. R.; Ballardini, R.; Balzani, V.; Boyd, S. E.; Credi, A.; Gandolfi, M. T.; Gómez-López, M.; Iqbal, S.; Philp, D.; Preece, J. A.; Prodi, L.; Ricketts, H. G.; Stoddart, J. F.; Tolley, M. S.; Venturi, M.; White, A. J. P.; Williams, D. J. *Chem. Eur. J.* **1997**, *3*, 152−170 and references therein.

(2) (a) Chambron, J. C.; Dietrich-Buchecker, C. O.; Sauvage, J.-P. *Top. Curr. Chem.* **1993**, *165*, 131−162. (b) Amabilino, D. B.; Stoddart, J. F. *Chem. Rev.* **1995**, *95*, 2725−2828. (c) Jäger, R.; Vögtle, F. *Angew. Chem., Int. Ed. Engl.* **1997**, *36*, 930−944.

(3) For examples of rotaxane-based device-like systems, see: (a) Bissell, R. A.; Córdova, E.; Kaifer, A. E.; Stoddart, J. F. *Nature (London)* **1994**, *369*, 133−137. (b) Anelli, P.-L.; Asakawa, M.; Ashton, P. R.; Bissell, R. A.; Clavier, G.; Górski, R.; Kaifer, A. E.; Langford, S. J.; Mattersteig, G.; Menzer, S.; Philp, D.; Slawin, A. M. Z.; Spencer, N.; Stoddart, J. F.; Tolley, M. S.; Williams, D. J. *Chem. Eur. J.* **1997**, *3*, 1113−1135. (c) Martínez-Díaz, M.-V.; Spencer, N.; Stoddart, J. F. *Angew. Chem., Int. Ed. Engl.* **1997**, *36*, 1904−1907. (d) Murakami, H.; Kawabuchi, A.; Kotoo, K.; Kunitake, M.; Nakashima, N. *J. Am. Chem. Soc.* **1997**, *119*, 7605−7606.

(4) For some recent examples of rotaxanes from other research groups, see: (a) Li, Z.-T.; Stein, P. C.; Becher, J.; Jensen, D.; Mørk, P.; Svenstrup, N. *Chem. Eur. J.* **1996**, *2*, 624−633. (b) Solladié, N.; Chambron, J.-C.; Dietrich-Buchecker, C. O.; Sauvage, J.-P. *Angew. Chem., Int. Ed. Engl.* **1996**, *35*, 906−909. (c) Vögtle, F.; Dünnwald, T.; Händel, M.; Jäger, R.; Meier, S.; Harder, G. *Chem. Eur. J.* **1996**, *2*, 640−643. (d) Anderson, S.; Anderson, H. L. *Angew. Chem., Int. Ed. Engl.* **1996**, *35*, 1956−1959. (e) Hannak, R. B.; Farber, G.; Konrat, R.; Krautler, B. *J. Am. Chem. Soc.* **1997**, *119*, 2313−2314. (f) Leigh, D. A.; Murphy, A.; Smart, J. P.; Slawin, A. M. Z. *Angew. Chem., Int. Ed. Engl.* **1997**, *36*, 728−732.

(5) Schill, G. *Catenanes, Rotaxanes, and Knots*; Academic Press: New York, 1971.

(6) (a) Ashton, P. R.; Belohradsky, M.; Philp, D.; Stoddart, J. F. *J. Chem. Soc., Chem. Commun.* **1993**, 1269−1274. (b) Ashton, P. R.; Belohradsky, M.; Philp, D.; Spencer, N.; Stoddart, J. F. *J. Chem. Soc., Chem. Commun.* **1993**, 1274−1277. (c) Amabilino, D. B.; Ashton, P. R.; Belohradsky, M.; Raymo, F. M.; Stoddart, J. F. *J. Chem. Soc., Chem. Commun.* **1995**, 747−750. (d) Amabilino, D. B.; Ashton, P. R.; Belohradsky, M.; Raymo, F. M.; Stoddart, J. F. *J. Chem. Soc., Chem. Commun.* **1995**, 751−753. (e) Asakawa, M.; Ashton, P. R.; Iqbal, S.; Stoddart, J. F.; Tinker, N. D.; White, A. J. P.; Williams, D. J. *Chem. Commun.* **1996**, 483−486. (f) Ashton, P. R.; Ballardini, R.; Balzani, V.; Belohradsky, M.; Gandolfi, M. T.; Philp, D.; Prodi, L.; Raymo, F. M.; Reddington, M. V.; Spencer, N.; Stoddart, J. F.; Venturi, M.; Williams, D. J. *J. Am. Chem. Soc.* **1996**, *118*, 4931−4951. (g) Asakawa, M.; Ashton, P. R.; Ballardini, R.; Balzani, V.; Belohradsky, M.; Gandolfi, M. T.; Kocian, O.; Prodi, L.; Raymo, F. M.; Stoddart, J. F.; Venturi, M. *J. Am. Chem. Soc.* **1997**, *119*, 302−310. (h) Ashton, P. R.; Everitt, S. R. L.; Gómez-López, M.; Jayaraman, N.; Stoddart, J. F. *Tetrahedron Lett.* **1997**, *38*, 5691−5694. (i) Raymo, F. M.; Stoddart, J. F. *Pure Appl. Chem.* **1997**, *69*, 1987−1997.

S0002-7863(97)03127-2 CCC: $15.00
Published on Web 03/03/1998

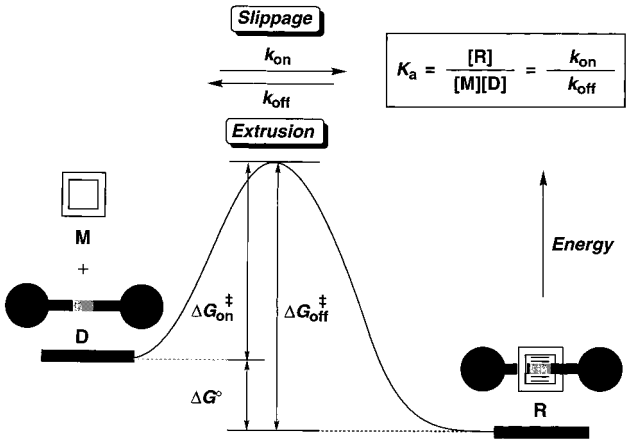

Figure 1. Schematic representation depicting the self-assembly of rotaxane-like entities using the slippage approach.

hydroquinone/dioxynaphthalene-based macrocycles (or "dumbbells") for the preparation of rotaxane-like species. We conjectured that we could self-assemble[9] rotaxane-like entities—employing the slippage approach—harnessing another recognition motif that we have employed for the noncovalent synthesis of pseudorotaxanes[10]—specifically, the interaction of secondary dialkylammonium ions with the commercially available macrocyclic polyether dibenzo[24]crown-8 (DB24C8).[11,12] By way of illustration, DB24C8 self-assembles with the dibenzylammonium ion ($\mathbf{1}^+$) to form (Scheme 1) a [2]pseudorotaxane superstructure that is stabilized primarily as a result of [N^+−H···O] and [C−H···O] hydrogen bonds, supplemented

Scheme 1. Self-Assembly of the Dibenzylammonium Ion ($\mathbf{1}^+$) with the Macrocyclic Polyether Dibenzo[24]crown-8 (DB24C8) To Form the [2]Pseudorotaxane [DB24C8·$\mathbf{1}$]$^+$

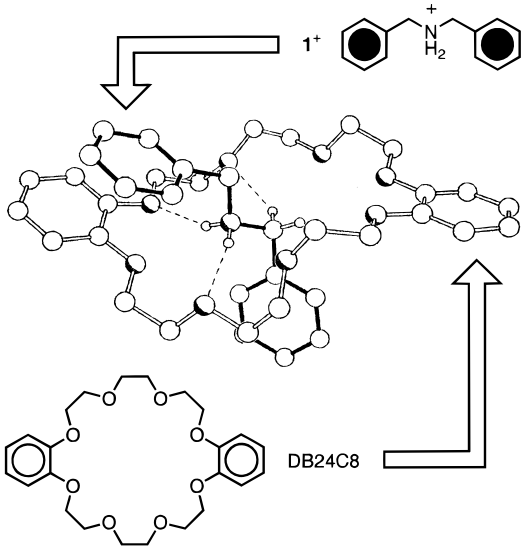

Scheme 2. Slippage-Type Synthesis of Rotaxane-like Systems by Using the Supramolecular Assistance To Synthesis Provided by Noncovalent Bonding Interactions between DB24C8 and Secondary Dialkylammonium Ions

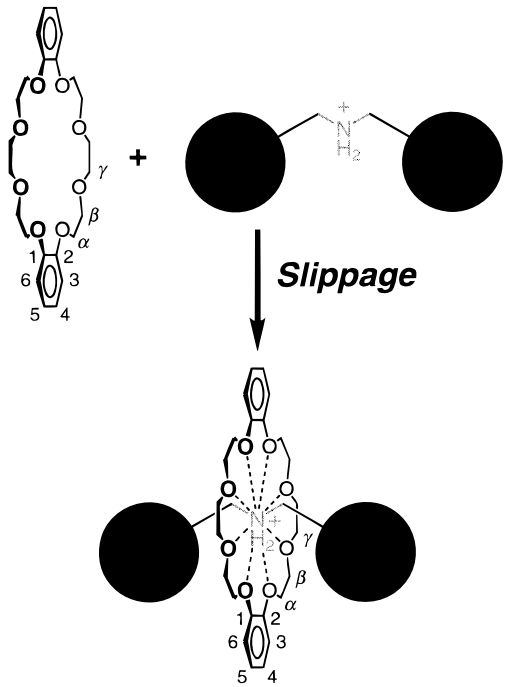

by $\pi-\pi$ stacking interactions. The $\mathbf{1}^+$ cation has some difficulty[11] threading its way through the DB24C8 macroring since its phenyl rings are relatively bulky compared to the size of the macrocycle's cavity. Hence, it seemed to us that we were very close to a situation where we could synthesize kinetically stable rotaxane-like species, via the slippage approach, utilizing the aforementioned DB24C8−dialkylammonium ion interactions (Scheme 2), i.e., we envisaged modifying the $\mathbf{1}^+$ cation slightly, so that we would reach a state where a dumbbell-like dialkylammonium ion ($\mathbf{D}^+$) would not form a complex with the beadlike crown ether DB24C8 at ambient temperature, but could be coaxed into forming a kinetically stable rotaxane-like entity under the influence of a suitable quantity of thermal energy. We visualized (Scheme 3) two possible modifications of the

(7) Prior to our research, rotaxane-like species had been synthesized statistically (i.e., involving methods in which noncovalent bonding interactions were not employed as a "synthetic aid") with slippage-type approaches. See: (a) Harrison, I. T. *J. Chem. Soc., Chem. Commun.* **1972**, 231−232. (b) Schill, G.; Beckmann, W.; Schweickert, N.; Fritz, H. *Chem. Ber.* **1986**, *119*, 2647−2655. However, in recent times, other researchers have also started to apply the slippage methodology using the supramolecular assistance to synthesis furnished by intermolecular interactions. See: (c) Macartney, D. H. *J. Chem. Soc., Perkin Trans. 2* **1996**, 2775−2778. (d) Händel, M.; Plevoets, M.; Gestermann, S.; Vögtle, F. *Angew. Chem., Int. Ed. Engl.* **1997**, *36*, 1199−1201.

(8) Fyfe, M. C. T.; Stoddart, J. F. *Acc. Chem. Res.* **1997**, *30*, 393−401.

(9) Philp, D.; Stoddart, J. F. *Angew. Chem., Int. Ed. Engl.* **1996**, *35*, 1154−1196.

(10) Pseudorotaxanes have been defined (Ashton, P. R.; Philp, D.; Spencer, N.; Stoddart, J. F. *J. Chem. Soc., Chem. Commun.* **1991**, 1677−1679) as the noninterlocked counterparts of rotaxanes, in which one or more linear "filaments" interpenetrate the cavities of one or more macrocyclic species to form inclusion complexes. Notably, as distinct from rotaxanes, these supramolecular complexes are free to dissociate into their separate components since they do not possess bulky stopper groups. For some recent examples, see: (a) Amabilino, D. B.; Anelli, P.-L.; Ashton, P. R.; Brown, G. R.; Córdova, E.; Godínez, L. A.; Hayes, W.; Kaifer, A. E.; Philp, D.; Slawin, A. M. Z.; Spencer, N.; Stoddart, J. F.; Tolley, M. S.; Williams, D. J. *J. Am. Chem. Soc.* **1995**, *117*, 11142−11170. (b) Ashton, P. R.; Langford, S. J.; Spencer, N.; Stoddart, J. F.; White, A. J. P.; Williams, D. J. *Chem. Commun.* **1996**, 1387−1388. (c) Baxter, P. N. W.; Sleiman, H.; Lehn, J.-M.; Rissanen, K. *Angew. Chem., Int. Ed. Engl.* **1997**, *36*, 1294−1296. (d) Mirzoian, A.; Kaifer, A. E. *Chem. Eur. J.* **1997**, *3*, 1052−1058. (e) Fyfe, M. C. T.; Glink, P. T.; Menzer, S.; Stoddart, J. F.; White, A. J. P.; Williams, D. J. *Angew. Chem., Int. Ed. Engl.* **1997**, *36*, 2068−2070.

(11) (a) Ashton, P. R.; Campbell, P. J.; Chrystal, E. J. T.; Glink, P. T.; Menzer, S.; Philp, D.; Spencer, N.; Stoddart, J. F.; Tasker, P. A.; Williams, D. J. *Angew. Chem., Int. Ed. Engl.* **1995**, *34*, 1865−1869. (b) Ashton, P. R.; Chrystal, E. J. T.; Glink, P. T.; Menzer, S.; Schiavo, C.; Spencer, N.; Stoddart, J. F.; Tasker, P. A.; White, A. J. P.; Williams, D. J. *Chem. Eur. J.* **1996**, *2*, 709−728. (c) Glink, P. T.; Schiavo, C.; Stoddart, J. F.; Williams, D. J. *Chem. Commun.* **1996**, 1483−1490.

(12) Utilizing this recognition motif, rotaxanes have been synthesized previously by a "threading followed by stoppering" approach. See: (a) Kolchinski, A. G.; Busch, D. H.; Alcock, N. W. *J. Chem. Soc., Chem. Commun.* **1995**, 1289−1291. (b) Ashton, P. R.; Glink, P. T.; Stoddart, J. F.; Tasker, P. A.; White, A. J. P.; Williams, D. J. *Chem. Eur. J.* **1996**, *2*, 729−736. (c) Reference 3c.

Scheme 3. Modifications to the $\mathbf{1}^+$ Cation Which Might Lead to Useful "Dumbbells" for a Slippage Synthesis of Rotaxane-like Species Involving DB24C8 and $(RCH_2)_2NH_2^+$ Ions

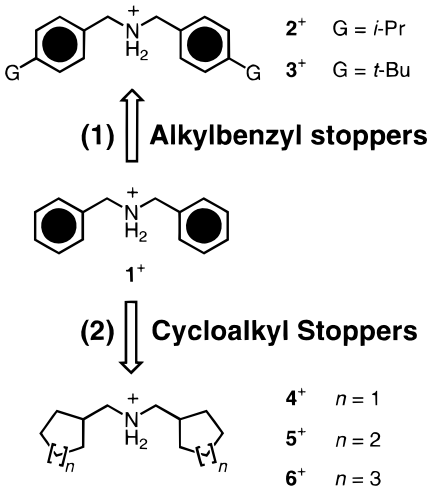

$\mathbf{1}^+$ cation for the synthesis of rotaxane-like structures using this approach. Either (1) bulky stopper groups could be placed at the termini of the cation $\mathbf{1}^+$, as in $\mathbf{2}^+$ or $\mathbf{3}^+$, whose phenyl rings are para-substituted with *i*-Pr and *t*-Bu groups, respectively, or (2) the $\mathbf{1}^+$ cation's phenyl rings could be replaced by fully saturated, more flexible—and hence, sterically more encumbering—cycloalkyl rings, as in $\mathbf{4}^+$, $\mathbf{5}^+$, or $\mathbf{6}^+$, where the phenyl rings have been exchanged for *c*-C_5H_9, *c*-C_6H_{11}, or *c*-C_7H_{13} rings, respectively. This article describes a systematic study of the complexation behavior of DB24C8 with the cations $\mathbf{2}^+$—$\mathbf{6}^+$ and reports the discovery of a 1:1 complex—formed between DB24C8 and the $\mathbf{5}^+$ cation—which is quite stable in nonpolar solvents that are reluctant to donate their nonbonding electrons into noncovalent bonds, i.e., those endowed with low Gutmann donor numbers (DN), but dissociates in polar solvents that are inclined to form such intermolecular bonds, i.e., those possessing a high DN.[13] Thus, we pose the following question—Is the $[DB24C8\cdot\mathbf{5}]^+$ complex a rotaxane, or is it a pseudorotaxane? We provide a fuzzy[14] answer which states that all pseudorotaxanes possess, to a certain extent, some rotaxane-like character.

Results and Discussion

Dumbbell Synthesis. The ammonium ions used in this investigation were prepared as their hexafluorophosphate salts to (1) augment their solubilities in organic solvents and (2) weaken ion pairing, i.e., to destabilize the reactants' ground-state energy compared to that of their complexes, thus making $\Delta G°$ more negative. The requisite secondary diamine precursors of the salts $\mathbf{2}\cdot PF_6$—$\mathbf{6}\cdot PF_6$ were prepared (Scheme 4) by two methods: specifically, by Route A—via a reductive amination sequence, in which the appropriate aldehyde and amine were condensed to produce an imine that was subsequently reduced with $NaBH_4$—and by Route B—via the condensation of the appropriate aldehyde with NH_3 and benzotriazole (BtH), followed by reduction of the resultant bis[1-(benzotriazol-1-yl)-alkyl]amine with $LiAlH_4$.[15] The secondary diamines obtained by these methods were then converted into the salts $\mathbf{2}\cdot PF_6$—$\mathbf{6}\cdot PF_6$ by heating with hydrochloric acid, followed by counterion exchange from chloride to hexafluorophosphate.

Scheme 4. Syntheses of the Secondary Dialkylammonium Salts $\mathbf{2}\cdot PF_6$—$\mathbf{6}\cdot PF_6$

Route A

R	Compound
p-*i*-PrC_6H_4	$\mathbf{2}\cdot PF_6$
p-*t*-BuC_6H_4	$\mathbf{3}\cdot PF_6$
c-C_6H_{11}	$\mathbf{5}\cdot PF_6$

Route B

R	Compound
c-C_5H_9	$\mathbf{4}\cdot PF_6$
c-C_7H_{13}	$\mathbf{6}\cdot PF_6$

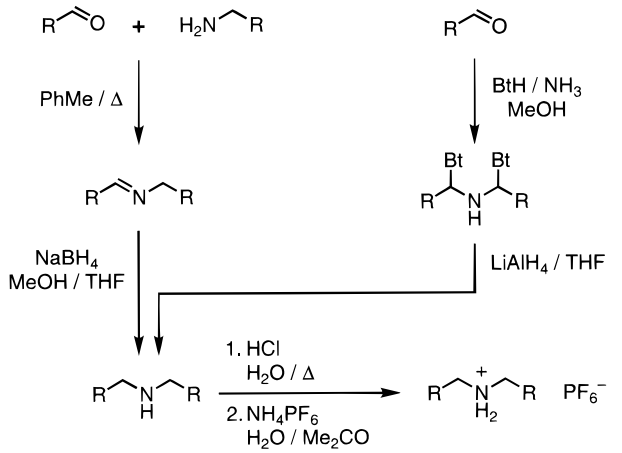

Pseudorotaxane Synthesis. We chose to monitor 1:1 complex formation by ^1H NMR spectroscopy, since the complexes formed between DB24C8 and secondary dialkylammonium ions tend to show[11] substantially different ^1H NMR spectra compared to those of the sum of their uncomplexed components. A $CDCl_3/CD_3CN$ (3:1) solvent system (hereinafter, for the sake of convenience, this mixed solvent system is referred to simply as MSS) was chosen to study the syntheses of the complexes: the $CDCl_3$ ensures[11] that the complexes will form with high stability constants (K_a), while the CD_3CN confers solubility upon the dialkylammonium salts.

A 1:1 mixture of DB24C8 and $\mathbf{2}\cdot PF_6$ was dissolved in the MSS. After 5 min, the room temperature ^1H NMR spectrum of this solution revealed (Figure 2a) no discernible complex formation. However, after a short period of time, the formation of additional peaks—corresponding to the $[DB24C8\cdot\mathbf{2}][PF_6]$ species—was noticed (Figure 2b). As time progressed, these peaks grew in intensity (Figure 2, parts c and d) so that the $[DB24C8\cdot\mathbf{2}]^+$ complex eventually developed into the dominant species present in solution. After ca. 9.5 days, equilibrium was attained, i.e., the rates of complexation and decomplexation became identical. Moreover, the same equilibrium position could be reached when a single crystal of the complex was dissolved in the MSS at 20 °C. Since the decomplexation process was observed at ambient temperature, the $[DB24C8\cdot\mathbf{2}]^+$ complex appears to be a *pseudorotaxane* and not a rotaxane. That is, the $\Delta G^{\ddagger}_{off}$ barrier is not large enough to prevent extrusion of the $\mathbf{2}^+$ ion from the $[DB24C8\cdot\mathbf{2}]^+$ species at 20 °C in the MSS. On the other hand, the *p*-*t*-BuC_6H_4 stopper groups of the dialkylammonium ion $\mathbf{3}^+$ are too bulky to permit the slippage of the DB24C8 macroring over them at various

(13) Previously,[11] we have noted that secondary dialkylammonium ions form the strongest complexes with DB24C8 in solvents possessing the lowest DNs, i.e., those lacking the ability to donate their electrons into noncovalent bonds.

(14) For excellent overviews describing the utility of fuzzy logic in chemistry, see: (a) Rouvray, D. H. *Chem. Br.* **1995**, *31*, 544—546. (b) Rouvray, D. H. *Chem. Ind. (London)* **1997**, 60—62.

(15) Katritzky, A. R.; Zhao, X.; Hitchings, G. J. *Synthesis* **1991**, 703—708.

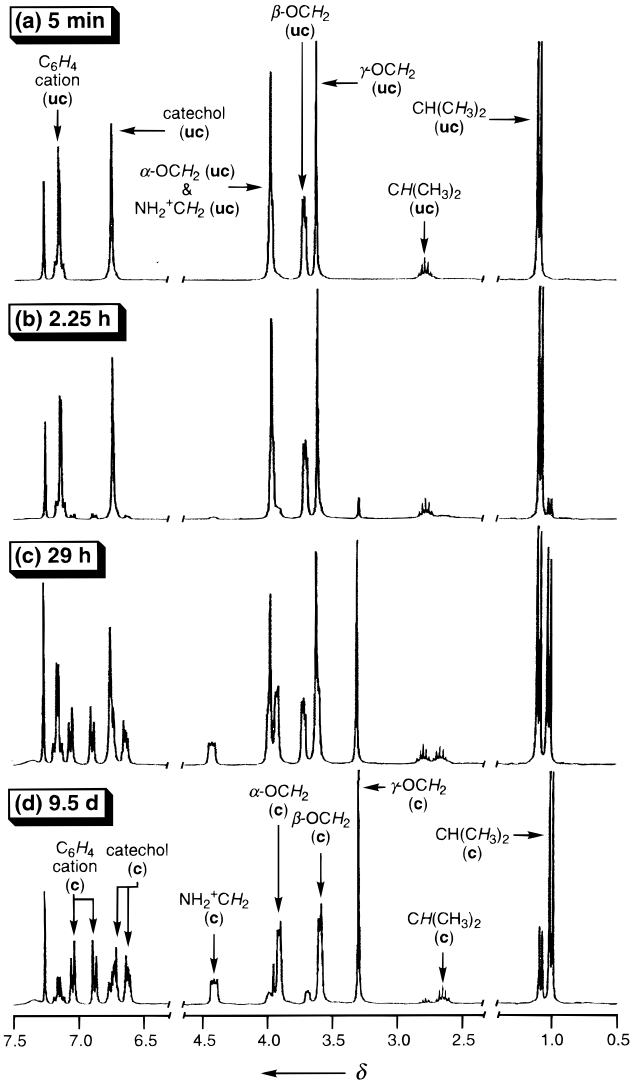

Figure 2. ^{1}H NMR spectra (MSS, 300.1 MHz, 20 °C) of a 1:1 mixture of DB24C8 and **2**·PF_6, illustrating the slow formation of the [DB24C8·**2**]-[PF_6] complex. The spectra portrayed were recorded after (a) 5 min, (b) 2.25 h, (c) 29 h, and (d) 9.5 days, respectively. Peaks associated with the uncomplexed crown ether and dialkylammonium ion are denoted by the descriptor **uc**, while those associated with the complex are denoted by the descriptor **c**. The initial concentrations of the crown ether and the salt were both 1.0×10^{-2} M. Chemical shift data for the compounds and complexes are listed in Table 1.

temperatures. In other words, DB24C8 and **3**·PF_6 coexist as two distinct chemical entities in solution, since only peaks for the uncomplexed polyether and salt were visible[16] in the ^{1}H NMR spectrum of a 1:1 mixture of DB24C8 and **3**·PF_6 in the MSS at 20 °C. Furthermore, this spectrum was not altered in the slightest when the solution was heated to 50 °C, i.e., even at elevated temperatures, the large $\Delta G^{\ddagger}_{on}$ barrier is insurmountable. This observation suggests that this system is extremely sensitive to steric effects:[17] the difference between the formation of a rotaxane-like species being detected or not corresponds to a simple change of stopper groups from *p*-*i*-PrC_6H_4 to *p*-*t*-BuC_6H_4. The sensitivity of this system may be ascribed to the (relatively) small and semirigid cavity of the DB24C8 macroring.

(16) See the Supporting Information for details.

(17) Hitherto, we have discovered[6a,f−g] slippage systems that are much less susceptible to steric effects. For instance, a much broader range of stopper groups can be used for slippage processes involving the larger and more flexible crown ether bis-*p*-phenylene[34]crown-10.

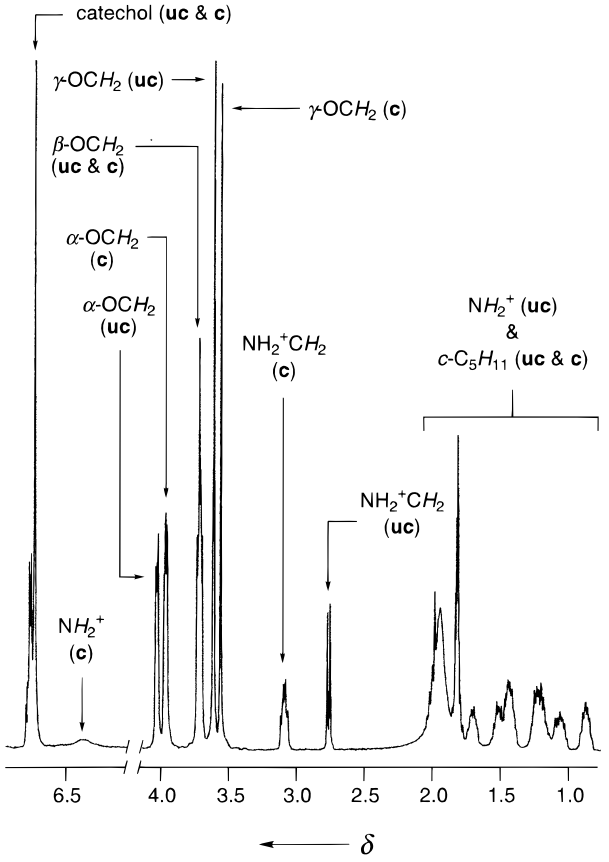

Figure 3. ^{1}H NMR spectrum (MSS, 400.1 MHz, 20 °C) of a 1:1 mixture of DB24C8 and **4**·PF_6 recorded 90 min after dissolution. The system has reached equilibrium, i.e., the relative intensities of the peaks for both the uncomplexed (**uc**) and complexed (**c**) species remain constant after this point. The initial concentrations of the macrocyclic polyether and the salt were both 1.0×10^{-2} M. Chemical shift data for the compounds and complexes are cataloged in Table 1.

At 20 °C, the equilibrium between the [DB24C8·**4**]$^+$ complex and its components was established by ^{1}H NMR spectroscopy (Figure 3) approximately 90 min after dissolving an equimolar mixture of DB24C8 and **4**·PF_6 in the MSS. Indeed, the slippage of the DB24C8 macroring over the *c*-C_5H_9 rings of the **4**$^+$ cation is so rapid that we were unable to obtain a ^{1}H NMR spectrum where only the free crown ether and the free salt could be observed at room temperature. Conversely, the ^{1}H NMR spectrum of a 1:1 solution (MSS) of DB24C8 and **5**·PF_6 at 20 °C showed (Figure 4a) peaks for the uncomplexed crown ether and salt only. Thus, there is clearly not enough thermal energy present at ambient temperature to permit the slippage of the DB24C8 macroring over the **5**$^+$ cation's *c*-C_6H_{11} groups such that the $\Delta G^{\ddagger}_{on}$ barrier can be surmounted. Encouragingly in this case, however, this barrier could be overcome at elevated temperatures. After the solution had been heated at 40 °C for ca. 16 weeks, a ^{1}H NMR spectrum was obtained (Figure 4b) that revealed the formation of a new complex. Inspired by this result, we sought a method by which this complex could be produced on a preparative scale. It appeared to us that CH_2Cl_2 was the solvent of choice, since it boils at 40 °C (so that temperature control of the reaction may be achieved simply by heating the reaction mixture under reflux) and has a low DN, thus permitting[11] the formation of strong rotaxane-like complexes. An indication that the ammonium-containing "dumbbell" **5**$^+$ was forming a complex with DB24C8, using this solvent as the reaction medium, was provided by the fact that the salt **5**·PF_6—which, under normal circumstances, is fairly

Table 1. ^{1}H NMR Data [δ Values] for Compounds and Complexes in the MSS[a]

	DB24C8				$(RCH_2)_2NH_2^+ PF_6^-$		
compd/complex	α-OCH_2[b]	β-OCH_2[b]	γ-OCH_2[b]	C_6H_4	CH_2[c]	*c*-C_nH_{2n-1}	*p*-C_6H_4-*i*-Pr
DB24C8	3.97	3.72	3.63	6.74			
2·PF_6					3.98		1.09, 2.78, 7.09−7.21
[DB24C8·**2**][PF_6]	3.92	3.59	3.30	6.57−6.66, 6.68−6.77	4.42		1.02, 2.66, 6.88, 7.05
4·PF_6					2.72	0.98−1.16, 1.41−1.64, 1.69−1.81, 1.85−2.12	
[DB24C8·**4**][PF_6]	4.04	3.74	3.57	6.77	3.10	0.80−0.96, 1.16−1.33, 1.41−1.64, 1.75−1.90	
5·PF_6					2.63	0.71−0.94, 0.97−1.21, 1.44−1.67	
[DB24C8·**5**][PF_6]	4.02	3.73	3.57	6.76	2.98	0.47−0.63, 0.65−0.90, 1.08−1.32, 1.33−1.48	

[a] The spectra were obtained at 20 °C on a Bruker AC300 spectrometer (at 300.1 MHz) or on a Bruker AMX400 spectrometer (at 400.1 MHz) with the deuterated solvent as the lock and the residual solvent as internal reference. [b] The descriptors α, β, and γ are defined in Scheme 2. [c] Methylene protons adjacent to the ammonium center.

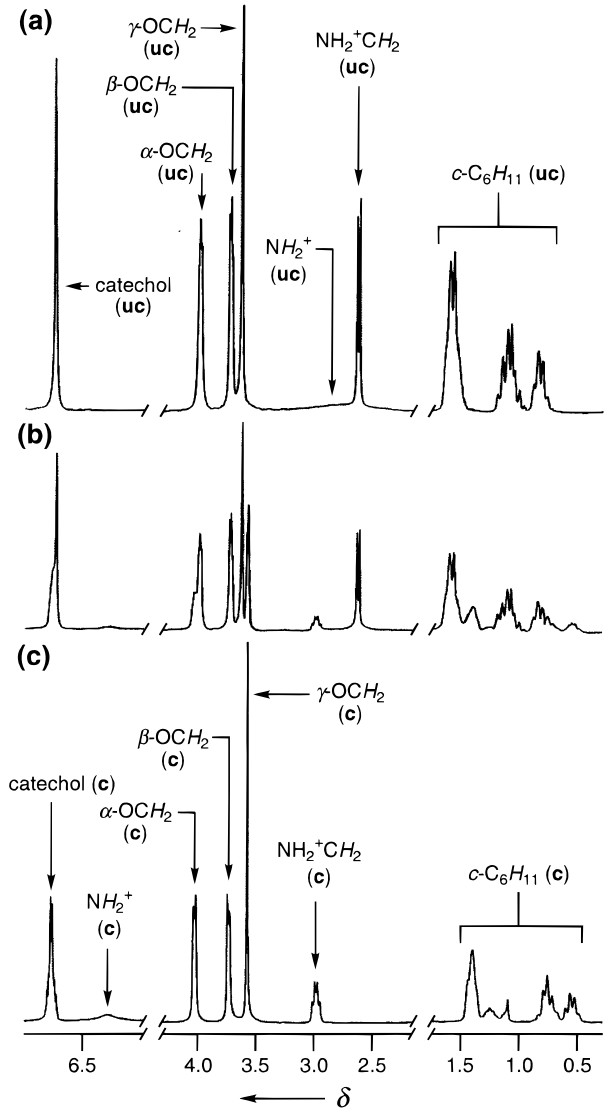

Figure 4. ^{1}H NMR spectra (MSS, 300.1 MHz, 20 °C) of (a) a 1:1 mixture of DB24C8 and **5**·PF_6 (both 1.0×10^{-2} M), (b) the same mixture after being heated at 40 °C for 16 weeks, and (c) the pure [DB24C8·**5**][PF_6] complex (1.0×10^{-2} M). Peaks associated with uncomplexed DB24C8 and $\mathbf{5}^+$ are indicated by the descriptor **uc**, while those associated with the [DB24C8·**5**]$^+$ complex are denoted by the descriptor **c**. Chemical shift data for the compounds and complexes are listed in Table 1.

insoluble in CH_2Cl_2—dissolved completely when it was heated under reflux in the presence of a 3-fold excess of the macrocyclic polyether for 4 days. Moreover, the ^{1}H NMR spectrum of the residue—produced after the solvent had been evaporated off from a small portion of the reaction mixture—recorded in the MSS, revealed the formation of the same species that had been generated in our earlier experiments. We used ^{1}H NMR spectroscopy to study the disappearance of the uncomplexed $\mathbf{5}^+$ cation and the appearance of its complex with DB24C8, which was shown (vide infra) to be the rotaxane-like complex [DB24C8·**5**]$^+$ by X-ray crystallography. By examining the relative intensities of the doublet[18] located at δ 2.63—corresponding to the $NH_2^+CH_2$ protons in the uncomplexed "dumbbell"—and the multiplet[18] situated at δ 2.98—arising from the $NH_2^+CH_2$ protons in the rotaxane-like complex—we were able to monitor (Table 2) the gradual buildup of the complex over a long period of time. Indeed, this experiment revealed that, after 36 days, almost 98% of the "dumbbell" had been converted[19] into its complex with DB24C8. Moreover, the complex could be easily isolated in 90% yield following a simple recrystallization procedure that employed a vapor diffusion technique. The ^{1}H NMR spectrum (Figure 4c) of the pure

Table 2. Conversion of **5**·PF_6 into [DB24C8·**5**][PF_6] upon Heating with a 3-Fold Excess of DB24C8 in CH_2Cl_2 at 40 °C[a]

time (days)	**5**·PF_6 (%)[b]	[DB24C8·**5**][PF_6] (%)[c]
0	100.0	0.0
4	63.5	36.5
8	43.5	56.5
12	30.6	69.4
16	18.6	81.4
20	11.0	89.0
24	7.5	92.5
28	4.6	95.4
32	3.3	96.7
36	2.2	97.8

[a] Reaction monitoring. A small portion of the reaction mixture was removed at the time stated. Thereupon, the solvent was evaporated off under reduced pressure, then the ^{1}H NMR spectrum of the residue was recorded in the MSS. The relative intensities of the peaks associated with the $NH_2^+CH_2$ protons for the uncomplexed and complexed **5**·PF_6 salt—which were observed at δ 2.63 and 2.98, respectively—were then evaluated. [b] Percentage amount of the uncomplexed **5**·PF_6 salt in the reaction mixture. [c] Percentage amount of the complexed **5**·PF_6 salt in the reaction mixture.

(18) In the free $\mathbf{5}^+$ cation, there is no coupling between the vicinal NH_2^+ and CH_2 protons since the NH_2^+ protons exchange with adventitious H_2O present in the solvent. On account of this exchange process, the signal for the CH_2 protons resonates as a doublet in the ^{1}H NMR spectrum of the uncomplexed cation. However, the crown ether's presence in the [DB24C8·**5**]$^+$ complex results in a cessation of the exchange process, so that the signal for the complex's $NH_2^+CH_2$ protons appears as a second-order multiplet presumably as a result of vicinal coupling between the two sets of protons.

[DB24C8·**5**][PF_6] complex revealed no dissociation in the MSS—even upon standing for several weeks at 20 °C. Nevertheless, the complex was not stable in all solvents at room temperature. When the [DB24C8·**5**][PF_6] complex was dissolved in $(CD_3)_2SO$—an electron-donating solvent that disrupts hydrogen bonding interactions and thus inhibits pseudorotaxane formation between DB24C8 and dialkylammonium ions[11]—at 25 °C, we noticed (Figure 5) that the signals associated with its $NH_2^+CH_2$ and OCH_2 protons progressively diminished in size with respect to the corresponding peaks identifiable with the uncomplexed cation and polyether, thus demonstrating that the complex can dissociate into its components—viz., DB24C8 and **5**·PF_6—under the appropriate conditions. After 18 h, complete extrusion of the $\mathbf{5}^+$ "dumbbell" from the complex was observed (Figure 5d).[20] This "schizophrenic" type of behavior raises the question—Is the [DB24C8·**5**][PF_6] complex a rotaxane, or is it a pseudorotaxane? At 20 °C, the complex is kinetically inert in the MSS, but it is kinetically labile in $(CD_3)_2SO$ since the free energy of activation for extrusion of the cation $\mathbf{5}^+$ becomes surmountable, in addition to the complex becoming less stable than its components. Thus, the [DB24C8·**5**][PF_6] complex appears to be a rotaxane when it is studied in nonpolar solvent systems, but manifests itself as either a pseudorotaxane or two distinct chemical species in polar solvents with high DNs.[21] By definition,[5] rotaxanes are compounds in which "bulky end groups prevent the extrusion of a threaded chain from a macrocycle". Therefore, the [DB24C8·**5**][PF_6] complex is a *pseudorotaxane*, and not a rotaxane, since its *c*-C_6H_{11} stoppers are not bulky enough to maintain its integrity under all circumstances. Where do we draw the line between rotaxanes and pseudorotaxanes, i.e., when does a complex stop being a pseudorotaxane and become a rotaxane? The best answer is obtained by employing a fuzzy[14] description of these systems, i.e., rather than impose an arbitrary and complicated cutoff parameter which distinguishes rotaxanes from pseudorotaxanes, it is best to say that the transition is a gradual one[22] in which pseudorotaxanes progressively acquire more rotaxane-like qualities until they are completely interlocked, as is observed in genuine rotaxanated structures. For instance, it can be seen that, as the cations' stopper groups are changed from *c*-C_5H_9 to *c*-C_6H_{11}, the rotaxane-like properties of the DB24C8-containing pseudorotaxanes are enhanced—at 20 °C, the [DB24C8·**4**]$^+$ complex dissociates in the MSS, while its *c*-C_6H_{11}-stoppered congener [DB24C8·**5**]$^+$ does not. Ultimately, to see if we could synthesize a system that possessed even more rotaxane-like character, we examined the DB24C8—**6**·PF_6 system. As we had observed with several of the systems studied earlier, the room temperature ^{1}H NMR spectrum[16] of a 1:1 mixture of DB24C8 and **6**·PF_6 exhibited signals which could only be attributed to the uncomplexed cation and crown ether. Similar to what had been observed previously with an equimolar mixture of DB24C8 and **3**·PF_6 (vide supra), the ^{1}H NMR spectrum of this solution was not altered, even upon heating to 50 °C, indicating that the *c*-C_7H_{13} stoppers are far too bulky to permit slippage of the DB24C8 macroring over them to form a rotaxane-like structure in this case. As before, this observation indicates that this system is highly susceptible to steric

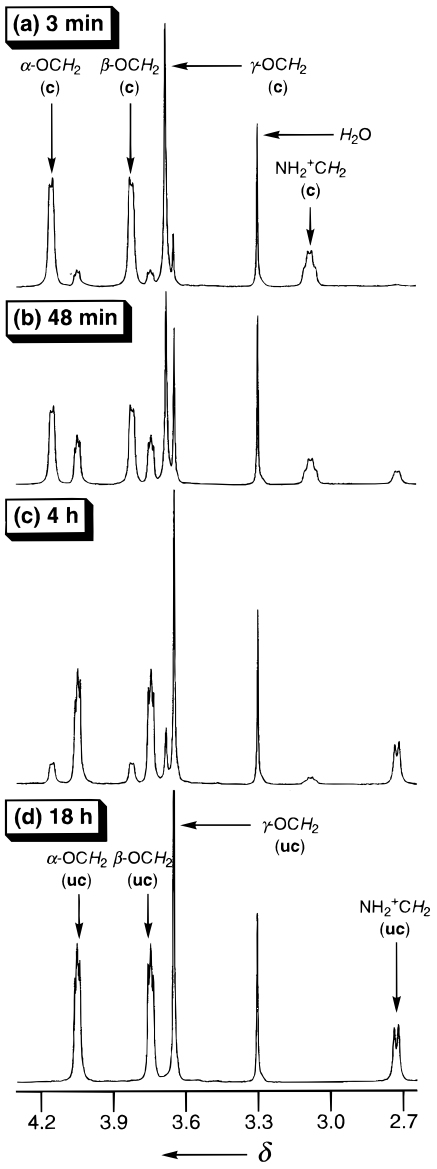

Figure 5. Partial ^{1}H NMR spectra ($(CD_3)_2SO$, 400.1 MHz, 25 °C) portraying the dissociation of the [DB24C8·**5**][PF_6] complex (initial concentration 1.0×10^{-2} M). The spectra illustrated were recorded after (a) 3 min, (b) 48 min, (c) 4 h, and (d) 18 h, respectively. Peaks associated with the complex are denoted by the descriptor **c**, while those associated with the uncomplexed crown ether and dialkylammonium ion are denoted by the descriptor **uc**.

(19) Further experimentation showed that the temperature and the presence of a large excess of DB24C8 were necessary to maximize the conversion of **5**·PF_6 into the [DB24C8·**5**][PF_6] complex. We observed only a 30% conversion of **5**·PF_6 into the complex when it was heated under reflux with DB24C8 (3 mol equiv) in $CHCl_3$—a solvent possessing a similar DN to CH_2Cl_2 but with a higher boiling point (61 °C). This observation is readily explained by Le Chatelier's principle, which states that the equilibrium is driven to the side of the reaction—in this case, the reactants—that absorbs energy upon heating. Moreover, this principle can also be used to explain the fact that we observed only an 88% conversion of the salt **5**·PF_6 into its DB24C8 complex when an equimolar mixture of the two components was heated under reflux in CH_2Cl_2 for 92 days.

(20) The first-order rate constant—calculated by using the integrated form of the first-order rate law and the ^{1}H NMR spectroscopic data—for the extrusion of the $\mathbf{5}^+$ cation from the [DB24C8·**5**][PF_6] complex was found to be 1.2×10^{-4} s^{-1} in $(CD_3)_2SO$ at 25 °C. This specific reaction rate corresponds to the complex having a half-life ($t_{1/2}$) of ca. 100 min in $(CD_3)_2SO$ at 25 °C.

(21) In many respects, systems such as these may be likened to "molecular locks" (Fujita, M.; Ibukuro, F.; Yamaguchi, K.; Ogura, K. *J. Am. Chem. Soc.* **1995**, *117*, 4175−4176) which have been described for systems that exploit the reversibility of coordinate covalent bonds between metals and ligands. In this instance, the overall bond (equivalent to the sum of the noncovalent and mechanical bonding interactions present) "locking" the DB24C8 macroring and the "dumbbell" $\mathbf{5}^+$ together is stable in low donicity solvents—however, this "lock" is "released" in high donicity solvents.

(22) It should be noted that the demeanor of this transitional phase will vary with solvent and temperature, i.e., the degree of rotaxane-like characteristics that a particular species is endowed with depends strongly upon the external conditions it experiences.

Table 3. Kinetic and Thermodynamic Data for the Syntheses[a] of the [2]Pseudorotaxanes [DB24C8·**2**][PF_6], [DB24C8·**4**][PF_6] and [DB24C8·**5**][PF_6], in the MSS at Various Temperatures

complex	temp (°C)	K_a $(M^{-1})^b$	$-\Delta G°$ (kcal $mol^{-1})^c$	k_{on} $(M^{-1}\ s^{-1})^d$	$\Delta G^{‡}_{on}$ (kcal $mol^{-1})^f$	k_{off} $(s^{-1})^e$	$\Delta G^{‡}_{off}$ (kcal $mol^{-1})^f$	probe protons[g]
[DB24C8·**2**][PF_6]	20	2870	4.6	1.1×10^{-3}	21.1	3.9×10^{-7}	25.7	C*H*Me_2
[DB24C8·**2**][PF_6]	40	2470	4.9	3.2×10^{-3}	21.9	1.3×10^{-6}	26.8	C*H*Me_2
[DB24C8·**4**][PF_6]	20	290	3.3	8.2×10^{-2}	18.6	2.8×10^{-4}	21.9	C*H*$_2NH_2^+$
[DB24C8·**4**][PF_6]	40	110	2.9	1.4×10^{-1}	19.6	1.3×10^{-3}	22.5	C*H*$_2NH_2^+$
[DB24C8·**5**][PF_6]	40	110	2.9	2.9×10^{-5}	24.9	2.6×10^{-7}	27.8	C*H*$_2NH_2^+$

[a] The reactions were followed with ^{1}H NMR spectroscopy by monitoring the changes in the relative intensities of the signals associated with the probe protons in the complexed and uncomplexed ammonium ions. [b] The K_a values were obtained from single-point measurements of the concentrations of the complexed and uncomplexed cations, in the relevant ^{1}H NMR spectrum, by using the expression K_a = [DB24C8·cation·PF_6]/[DB24C8][cation·PF_6]. [c] The free energies of association ($\Delta G°$) were calculated from the K_a values by using the expression $\Delta G° = -RT \ln K_a$. [d] The second-order rate constants for the slippage processes (k_{on}) were calculated employing eq 1. [e] The first-order rate constants for the extrusion processes (k_{off}) were calculated from the k_{on} and K_a values by using the expression $k_{off} = k_{on}/K_a$. [f] The free energies of activation for the slippage ($\Delta G^{‡}_{on}$) and extrusion ($\Delta G^{‡}_{off}$) processes were calculated by using the relationships $\Delta G^{‡}_{on} = -RT \ln(k_{on}h/\boldsymbol{k}T)$ and $\Delta G^{‡}_{off} = -RT \ln(k_{off}h/\boldsymbol{k}T)$, respectively, where R, h and $\boldsymbol{k}$ correspond separately to the gas, Planck and Boltzmann constants. [g] Probe protons located on the ammonium ion.

effects[17]—slippage of the DB24C8 macroring over the stopper units of the dialkylammonium ions rapidly becomes more difficult as more CH_2 groups are inserted into the cations' cycloalkyl termini.

The chemical shift data for the pseudorotaxanes and their components are presented in Table 1. In general, downfield shifts were observed for the resonances associated with the ammonium ions' protons upon complexation, the largest shifts being exhibited by the methylene protons adjacent to the ammonium center. For the most part, the proton resonances associated with the DB24C8 macroring were shifted to a lesser extent than their counterparts on the ammonium ions.

Thermodynamics and Kinetics of Pseudorotaxane Formation. The absolute concentrations of the uncomplexed crown ether/salts and their associated pseudorotaxane complexes can be calculated[11] from the known original concentrations of DB24C8 and the ammonium salts, in addition to the relative intensities of the ^{1}H NMR signals associated with each species. Hence, at equilibrium, the observation of both complexed and uncomplexed species in solution provides a suitable single-point determination[23] of the complexes' K_a values (Table 3) and their derived free energies of complexation ($\Delta G°$). Not surprisingly, the [DB24C8·**2**][PF_6] complex possesses the highest K_a values, probably as a result of the greater acidity of the benzylic CH_2 protons with respect to their cycloalkyl CH_2 counterparts, in addition to the presence of supplementary stabilizing aryl−aryl stacking interactions. Noticeably, in all cases, the K_a values decrease at higher temperatures, an effect that may be rationalized utilizing Le Chatelier's principle, i.e., at higher temperatures, the equilibrium is shifted toward the species that absorbs energy.

To examine the kinetic parameters associated with these systems, pseudorotaxane formation was studied by ^{1}H NMR spectroscopy at 20 and 40 °C in the MSS. By monitoring the decrease in the relative intensities of the ^{1}H NMR signals associated with various probe protons in the free dialkylammonium ions with respect to their concomitant appearance in the complexes with time, we could calculate (Table 3) the rate constants for the slippage processes, k_{on}, using eq 1:[24]

$$P_t = [D_0^2 P_e e^{(k_{on}t(D_0^2 - P_e^2)/P_e)} - D_0^2 P_e]/[D_0^2 e^{(k_{on}t(D_0^2 - P_e^2)/P_e)} - P_e^2] \quad (1)$$

where D_0 corresponds to the initial concentration of the uncomplexed dialkylammonium salts or macrocyclic polyether, while P_e and P_t are commensurate with the concentration of the pseudorotaxanes at equilibrium and at time, t, respectively. Nonlinear curve fitting of the plot of P_t against t furnished values of k_{on} from which estimations of the respective free energies of activation for slippage ($\Delta G^{‡}_{on}$) and extrusion ($\Delta G^{‡}_{off}$) could be determined (Table 3). As anticipated from previous experiments, the free energy of activation for the slippage of the DB24C8 macroring over the dialkylammonium ions' stopper groups, viz., $\Delta G^{‡}_{on}$, increases in the series $\mathbf{4}^+ < \mathbf{2}^+ < \mathbf{5}^+$, indicating that it is relatively easy for DB24C8 to slip over *c*-C_5H_9 rings, while it is much more difficult for it to slip over *c*-C_6H_{11} rings. Moreover, the free energy of extrusion, viz., $\Delta G^{‡}_{off}$, also increases in the same series. Since this value is a measure of the kinetic stability of the pseudorotaxane supermolecules in the MSS—*i.e.*, it represents a barrier that must be overcome for complex dismemberment to occur—we can say that the [DB24C8·**5**]$^+$ species has more rotaxane-like character than the [DB24C8·**2**]$^+$ species, which, in turn, has more rotaxane-like character than the [DB24C8·**4**]$^+$ system.

Table 4. LSIMS Data[a] for DB24C8−Secondary Dialkylammonium Salt (**D**·PF_6) Mixtures and Crystals of Their Associated Pseudorotaxanes

mixture or complex	*m*/*z* $\mathbf{D}^{+}$ [d]	*m*/*z* [DB24C8·**D**]$^+$ [e](%)[f]
DB24C8 + **2**·PF_6[b]	282	730 (10)
[DB24C8·**2**][PF_6][c]	282	730 (667)
DB24C8 + **3**·PF_6[b]	310	758 (6)
DB24C8 + **4**·PF_6[b]	182	630 (145)
[DB24C8·**4**][PF_6][c]	182	630 (149)
DB24C8 + **5**·PF_6[b]	210	658 (7)
[DB24C8·**5**][PF_6][c]	210	658 (250)
DB24C8 + **6**·PF_6[b]	238	687 (3)

[a] LSIMS spectra were obtained by using a VG Zabspec mass spectrometer equipped with a cesium ion source and utilizing a *m*-nitrobenzyl alcohol matrix. [b] Equimolar mixture of DB24C8 and dialkylammonium salt. [c] Crystals of pseudorotaxane. [d] $(M - PF_6)^+$ peak corresponding to the uncomplexed dialkylammonium ion $\mathbf{D}^+$. [e] $(M - PF_6)^+$ peak corresponding to a DB24C8−dialkylammonium ion complex [DB24C8·**D**]$^+$. [f] Relative intensity of the [DB24C8·**D**]$^+$ peak compared to the $\mathbf{D}^+$ peak expressed as a percentage.

Mass Spectrometry. Data acquired from the liquid secondary ion mass spectra (LSIMS) of 1:1 mixtures of DB24C8 and the secondary dialkylammonium salts (**D**·PF_6), in addition to the LSIMS data for cocrystals of some of the DB24C8−dialkylammonium salt complexes, are displayed in Table 4. In all instances, the peaks observed for the uncomplexed macrocyclic polyether were very small and insignificant[25] compared

(23) Adrian, J. C., Jr.; Wilcox, C. S. *J. Am. Chem. Soc.* **1991**, *113*, 678−680 and references therein.

(24) This equation was derived[16] from the integrated rate equation for an equilibrating reaction between two reactants—in this instance, DB24C8 and the dialkylammonium ion—and a single product—here, the 1:1 pseudorotaxane complex formed between DB24C8 and the dialkylammonium ion.

to the peak for the uncomplexed ammonium ions $\mathbf{2}^+$−$\mathbf{6}^+$. However, several important features became evident when we examined the relative intensities of the peaks associated with the uncomplexed ammonium ions and their DB24C8 complexes. Only in the case of the [DB24C8·**4**]$^+$ complex were peaks of approximately the same intensity detected for (1) a 1:1 DB24C8−secondary dialkylammonium salt mixture[26] and (2) cocrystals[26] of the corresponding pseudorotaxane, indicating that the "gas phase" rates of complexation and decomplexation are both relatively fast for this system. On the other hand, vast differences were noted between (1) the LSIMS of 1:1 mixtures[26] of DB24C8 with the salts **2**·PF_6 and **5**·PF_6 and (2) the LSIMS of crystals[26] of the corresponding 1:1 complexes, viz., [DB24C8·**2**][PF_6] and [DB24C8·**5**][PF_6]. The [DB24C8·**2**]$^+$ and [DB24C8·**5**]$^+$ peaks observed in the LSIMS spectra of 1:1 mixtures[26] of DB24C8 with either **2**·PF_6 or **5**·PF_6—i.e., systems in which no 1:1 complexes were present initially—were infinitesimal compared to the signals retrieved from their associated cocrystals.[26] This observation indicates that these systems' complexation/decomplexation rates are exceptionally slow during their flight through the mass spectrometer. Equimolar mixtures[26] of DB24C8 with the salts **3**·PF_6 and **6**·PF_6—salts which were shown (vide supra) not to form complexes with DB24C8 under any circumstances in solution—exhibit LSIMS which display very weak signals for the 1:1 DB24C8−dialkylammonium ion complexes. These very weak signals presumably arise as a result of a small amount of "face-to-face" complexation between the ammonium ions and the macrocyclic polyether in the "gas phase". Interestingly, these signals were smaller than those detected in the LSIMS of 1:1 mixtures of DB24C8 with either **2**·PF_6 or **5**·PF_6, perhaps indicating that there is a certain degree of formation of [DB24C8·**2**]$^+$ or [DB24C8·**5**]$^+$ pseudorotaxane superstructures in the "gas phase".

X-ray Crystallography. The X-ray analysis of the 1:1 pseudorotaxane complex formed between the $\mathbf{2}^+$ cation and DB24C8 reveals (Figure 6) a structure that has a co-conformation[27] very similar to that observed (cf. Scheme 1) for the related [DB24C8·**1**]$^+$ complex.[11] The DB24C8 macrocycle adopts an extended, approximately C_i-symmetric conformation reminiscent of that observed[28] in its uncomplexed state, i.e., its two catechol rings retain coplanarity with their adjoining OCH_2CH_2 fragments. One of the phenylene rings of the cation is positioned over one of the catechol rings of the DB24C8 macroring (mean interplanar separation 3.56 Å, centroid−centroid distance 4.38 Å, the rings being inclined by ca. 14° to one another), while the other phenylene ring is oriented approximately axially to this macrocycle.[29] Complex stabilization is achieved via $\pi-\pi$ stacking interactions (vide supra) and a combination of both [N^+−H···O] and [C−H···O] hydrogen bonds (Figure 6). Inspection of the packing of the [DB24C8·**2**]$^+$ pseudorotaxane supermolecules does not reveal any additional intercomplex interactions in the crystal.

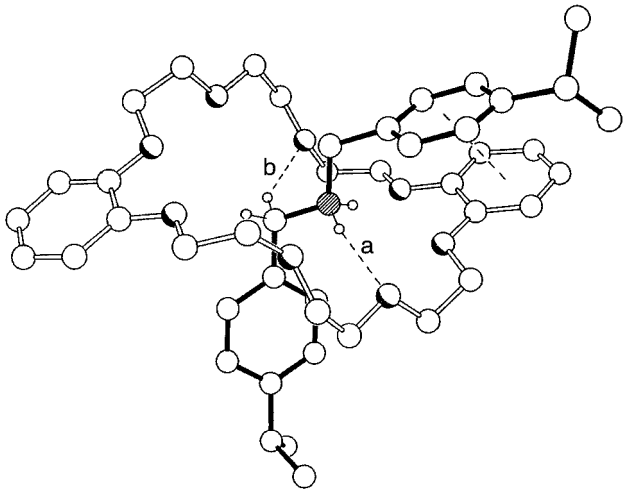

Figure 6. The solid-state superstructure of the [2]pseudorotaxane [DB24C8·**2**][PF_6]. The hydrogen bonding geometries are (a) [N^+···O], [H···O] 2.96, 2.11 Å, [N^+−H···O] 158° and (b) [C···O], [H···O], 3.26, 2.43 Å, [C−H···O] 145°.

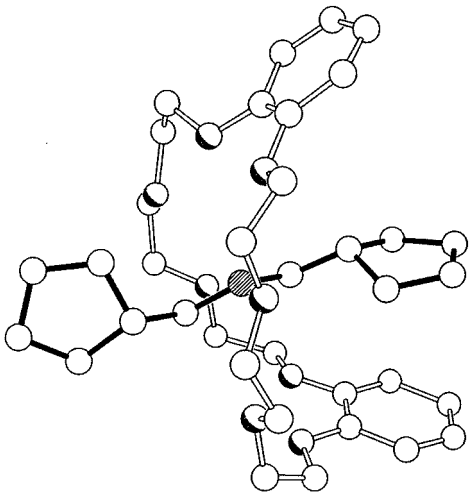

Figure 7. The solid-state superstructure of one of the two crystallographically independent [2]pseudorotaxanes present in the crystals of [DB24C8·**4**][PF_6].

The solid state superstructure of the 1:1 pseudorotaxane complex is markedly altered on changing the cation from one containing substituted benzyl groups, attached to the NH_2^+ center, to one carrying cyclopentylmethyl substituents. In this instance (Figure 7), the DB24C8 macroring adopts a folded, V-shaped conformation, with the cation inserted approximately axially through its center. The crystals contain two crystallographically independent [DB24C8·**4**]$^+$ pseudorotaxanes, both with very similar co-conformations.[27] The "cleft angles" between the two catechol rings in the two complexes are 47 and 50°, respectively. The cations' $CHCH_2NH_2^+CH_2CH$ backbones both have all-anti geometries and are slipped such that, in each case, the nitrogen atoms lie ca. 0.6 Å from the centroid of the eight polyether oxygen atoms. The centroid−

(25) This feature of the LSIMS arises since the dialkylammonium ions are already charged and do not need to be ionized before they are desorbed into the "gas phase" from the matrix. On the other hand, the neutral crown ether molecules are not desorbed to such a great extent since they must be ionized beforehand.

(26) In solvent-free 1:1 mixtures of DB24C8 and the $(RCH_2)_2NH_2$·PF_6 salts, no pseudorotaxane complexes are present originally—the only chance that the compounds have to form pseudorotaxanes, prior to desorption, occurs when they are dissolved in the matrix. Consequently, the pseudorotaxane content of samples produced from DB24C8−$(RCH_2)_2NH_2$·PF_6 mixtures may be considered to be negligible before desorption. On the other hand, cocrystals of DB24C8 with the salts—isolated after the components had been allowed to equilibrate completely—may be considered to consist of pure pseudorotaxane, as verified by X-ray crystallographic analysis (vide supra).

(27) Strictly speaking, the term "conformation" refers only to the three-dimensional spatial organization of atoms in discrete molecular species that are interconvertible merely by free rotation about chemical bonds. Accordingly, we have adopted[10e] the expression "co-conformation" to designate the three-dimensional spatial arrangement of the atoms in supramolecular systems that can be interconverted by bond rotation.

(28) Hanson, I. R.; Hughes, D. L.; Truter, M. R. *J. Chem. Soc., Perkin Trans. 2* **1976**, 972−978.

(29) Stronger $\pi-\pi$ stacking interactions between the two aromatic systems are probably precluded by the bulky *i*-Pr substituent.

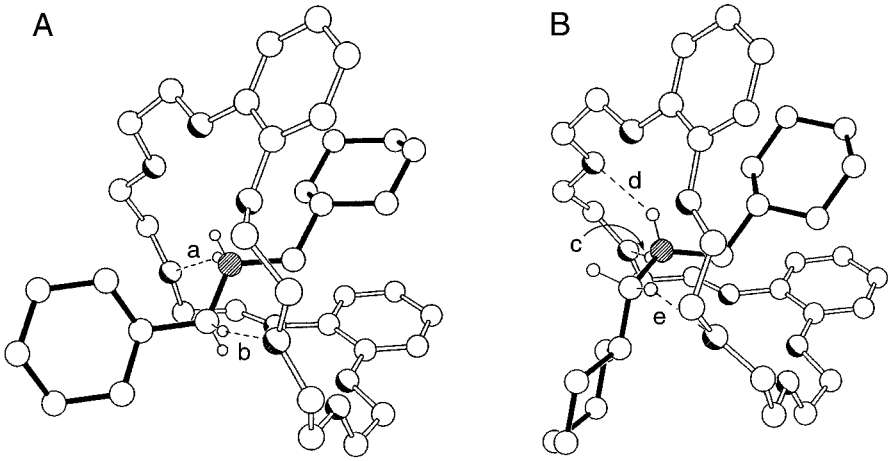

Figure 8. The two crystallographically independent 1:1 complexes [DB24C8·**5**][PF_6]. In complex **A**, the hydrogen bonding geometries are (a) [N^+···O], [H···O] 3.05, 2.20 Å, [N^+−H···O] 156° and (b) [C···O], [H···O] 3.30, 2.35 Å, and [C−H···O] 170°. In complex **B**, the hydrogen bonding geometries are (c) [N^+···O], [H···O] 2.89, 2.01 Å, [N^+−H···O] 165°, (d) 2.87, 2.24 Å, 126°, and (e) [C···O], [H···O] 3.14, 2.27 Å [C−H···O] 151°.

Table 5. Crystal Data, Data Collection, and Refinement Parameters[a]

data	[DB24C8·**2**][PF_6]	[DB24C8·**4**][PF_6]	[DB24C8·**5**][PF_6]
formula	$C_{44}H_{60}NO_8$·PF_6	$C_{36}H_{56}NO_8$·PF_6	$C_{38}H_{60}NO_8$·PF_6
solvent	0.25 C_6H_{14}		
formula wt	897.4	775.8	803.8
color, habit	clear prisms	clear needles	clear prisms
crystal size/mm	0.77 × 0.70 × 0.60	1.00 × 0.40 × 0.17	0.47 × 0.43 × 0.40
lattice type	monoclinic	orthorhombic	orthorhombic
space group symbol, no.	$P2_1/n$, 14	*Pbca*, 61	*Pbca*, 61
cell dimensions			
a/Å	12.202(3)	16.264(1)	16.539(1)
b/Å	10.749(1)	30.838(2)	31.722(3)
c/Å	40.325(4)	32.173(4)	32.130(2)
β/deg	98.60(1)		
V/Å^3	5230(1)	16137(3)	16857(2)
Z	4	16[b]	16[b]
D_c/g cm^{-3}	1.140	1.277	1.267
F(000)	1906	6592	6848
μ/mm^{-1}	1.04	1.26	1.23
θ range/deg	2.2−55.0	2.8−55.0	2.8−60.0
no. of unique reflcns			
measd	6490	10142	12308
obsd, $\lvert F_o\rvert > 4\sigma(\lvert F_o\rvert)$	2589	4803	4832
no. of variables	638	618	641
R_1[c]	0.114	0.146	0.197
wR_2[d]	0.309	0.376	0.539
weighting factors *a*, *b*[e]	0.246, 0.000	0.215, 71.165	0.415, 25.238
largest difference peak, hole/eÅ^{-3}	0.73, −0.27	0.68, −0.45	0.78, −0.57

[a] Details in common: graphite monochromated Cu Kα radiation, ω-scans, Siemens P4 diffractometer, 293 K, refinement based on F^2. [b] There are two crystallographically independent molecules in the asymmetric unit. [c] $R_1 = \Sigma||F_o| - |F_c||/\Sigma|F_o|$. [d] $wR_2 = \{\Sigma[w(F_o^2 - F_c^2)^2]/\Sigma[w(F_o^2)^2]\}^{1/2}$ [e] $w^{-1} = \sigma^2(F_o^2) + (aP)^2 + bP$.

centroid distances between the *c*-C_5H_9 rings and their associated "sandwiching" catechol units are 4.26 and 4.67 Å in one complex, while they are 4.37 and 4.74 Å in the other. There is a marked absence of any strong [N^+−H···O] or [C−H···O] hydrogen bonding interactions. The shortest respective [N···O] distances are 3.04 and 3.08 Å in the two complexes, but the closest approaches of any of the NH_2^+ hydrogen donors to any potential DB24C8 oxygen acceptors are all greater than 2.3 Å. Similarly, the shortest contact from either of the cations' $NH_2^+CH_2$ hydrogen atoms to the polyether oxygen atoms is 2.44 Å. As was the case with the [DB24C8·**2**]$^+$ complex, there are no intercomplex interactions of any note.

In the solid-state superstructure of the [2]pseudorotaxane [DB24C8·**5**]$^+$, there are also two crystallographically independent 1:1 complexes in the asymmetric unit. Although the DB24C8 macrocycle adopts a folded, V-shaped conformation in both cases, with respective "cleft angles" of 57 and 55°, the co-conformations[27] and geometries of the binding of the cations differ markedly in each case. In one of the complexes, the geometries about the two C−N bonds within the cation are anti, whereas in the other, the geometry about one of these bonds is gauche. In both independent complexes, one of the *c*-C_6H_{11} rings is sandwiched between the catechol rings of the DB24C8 macrocycle with ring-centroid−ring-centroid separations of 4.39 and 4.69 Å in one complex and 4.49 and 4.70 Å in the other. In both pseudorotaxane complexes, there are distinct [N^+−H···O] and [C−H···O] stabilizing interactions (Figure 8). As with the previous two complexes, there are no notable interpseudorotaxane interactions.

The crystal data, data collection and refinement parameters for the crystal structures reported in this article are summarized in Table 5.

Molecular Modeling. To gain further insight into the size complementarity requirements associated with the slippage processes, the passage of the macrocyclic polyether over the terminal aryl or cycloalkyl groups of the dumbbell-like com-

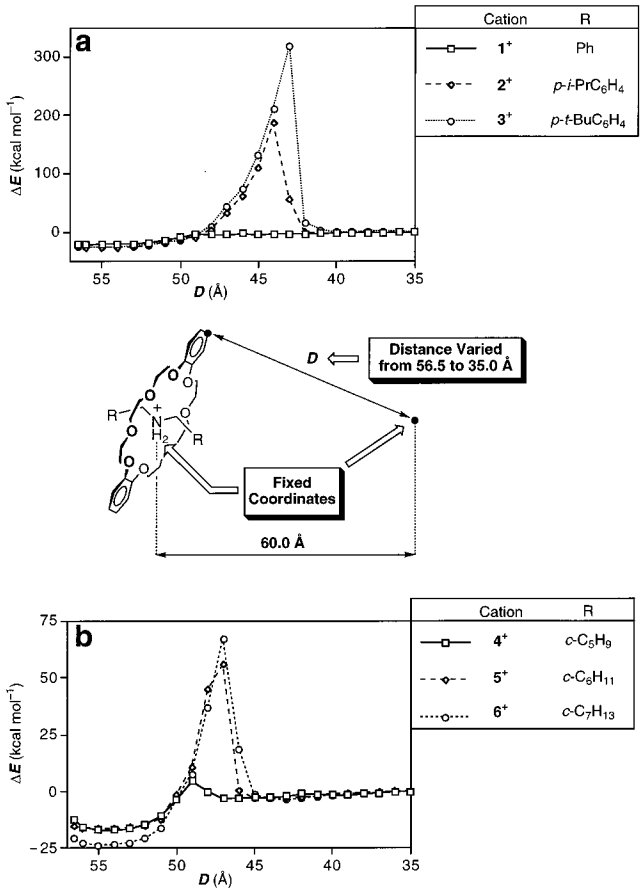

Figure 9. Schematic diagram illustrating the protocol utilized for the computational simulations delineated in this article, in addition to energy profiles associated with the passage of the macrocyclic polyether DB24C8 over the (a) terminal aryl groups of the cationic "dumbbells" $\mathbf{1}^+-\mathbf{3}^+$ and (b) cycloalkyl termini of the dumbbell-like cations $\mathbf{4}^+-\mathbf{6}^+$.

ponents $\mathbf{1}^+-\mathbf{6}^+$ was simulated computationally. In particular, the preformed complexes—constructed within the input mode of Macromodel[30] 5.0—were employed as the simulations' initial geometries. In each case, the distance, *D* (Figure 9), separating the carbon atom in position 4 of one of the macrocyclic polyether's two catechol rings and a reference "dummy" atom—located at a distance of 60.0 Å from the nitrogen atom—was reduced stepwise from 56.5 to 35.0 Å. As a result, the macrocycle was forced to move along the dumbbell-like component, eventually passing over one of its two termini. An energy minimization was performed at each step—this step's initial geometry coincided with the previous step's final geometry. The energies obtained for each step were "normalized" by subtracting the concluding step's energy—corresponding to the energy associated with the well-separated macrocyclic and dumbbell-like components—from each value. The resulting energy differences ΔE were plotted against the values of *D* to furnish the energy profiles illustrated in Figure 9. In the case of the dumbbell-like cation $\mathbf{1}^+$ (Figure 9a)—i.e., when R is equal to Ph—the energy profile is remarkably "flat". However, by increasing the size of R—i.e., by replacing Ph for *p*-*i*-PrC_6H_4 and *p*-*t*-BuC_6H_4 in $\mathbf{2}^+$ and $\mathbf{3}^+$, respectively—pronounced energy barriers were observed at *D* values of 44.0 and 43.0 Å, for $\mathbf{2}^+$ and $\mathbf{3}^+$, individually. Similarly, in the case of the dumbbell-like cations $\mathbf{4}^+-\mathbf{6}^+$, incorporating terminal cycloalkyl groups,

(30) Mahamadi, F.; Richards, N. G. K.; Guida, W. C.; Liskamp, R.; Lipton, M.; Caufield, D.; Chang, G.; Hendrickson, T.; Still, W. C. *J. Comput. Chem.* **1990**, *11*, 440−467.

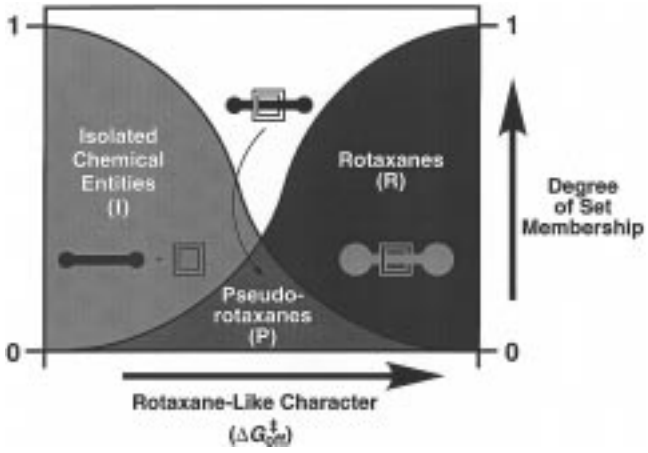

Figure 10. Schematic illustration, indicating that pseudorotaxanes are represented by the intersection set [**R** ∩ **I**] of the sets of rotaxanes (**R**) and isolated chemical entities (**I**), i.e., the fuzzy domain between these two sets. Consequently, pseudorotaxanes are species that are endowed simultaneously with characteristics associated with species belonging to both **R** and **I**. The numbers 1 and 0 have been assigned arbitrarily to the respective species which belong either totally or not at all to the sets **R** and **I**.

the energy barrier associated with the passage of the macrocyclic component over one of the terminal cycloalkyl groups increases (Figure 9b) with the number of methylene groups incorporated within the cycloalkyl residues. In conclusion, for both the aryl- and cycloalkyl-terminated cations $\mathbf{1}^+-\mathbf{3}^+$ and $\mathbf{4}^+-\mathbf{6}^+$, respectively, the slippage of the macrocyclic component over the terminal groups becomes increasingly difficult as the size of these groups is enlarged. This trend is consistent (vide supra) with the experimental observations, both in solution and in the "gas phase". Nonetheless, the energy barriers derived from the substituted benzyl-terminated dumbbell-like cations $\mathbf{2}^+$ and $\mathbf{3}^+$ are significantly higher than those determined for their cycloalkyl-containing congeners $\mathbf{5}^+$ and $\mathbf{6}^+$. These findings are apparently in contrast with the experimental observations, which reveal (vide supra) that the macrocyclic polyether is able to pass over the *p*-*i*-PrC_6H_4 groups of $\mathbf{2}^+$, but not over the *c*-C_7H_{13} groups of $\mathbf{6}^+$—i.e., the free energy of activation associated with the slippage process, viz., $\Delta G^{\ddagger}_{on}$, is higher in the case of $\mathbf{6}^+$ than that of $\mathbf{2}^+$. This apparent contradiction is presumably a result of entropic effects, which are expected to be significant for the rather flexible cycloalkyl groups under the experimental conditions. However, the entropic term is not taken into account by the molecular mechanics calculations, since the calculated ΔE values can be equated, at best, with enthalpy differences at 0 K and not with free energy differences. Thus, the energy barriers obtained from these slippage simulations must be considered as *relative* measures, comparable only when *similar* dumbbell-like cations are being considered.

Conclusions

By modifying the termini of the cation $\mathbf{1}^+$, we have demonstrated that it is possible to synthesize rotaxane-like species—composed of DB24C8 and secondary dialkylammonium ions—which are kinetically stable under the appropriate conditions. In particular, we have shown that the [DB24C8·**5**]-[PF_6] complex is stable at ambient temperature in a solvent endowed with a low DN. "Under the appropriate conditions" is the key phrase in this instance, for the other rotaxane-like complexes which we have studied in this article will undoubtedly be kinetically stable at lower temperatures. These examples

serve to highlight the fact that the transformation from a pseudorotaxane into a rotaxane is a progressive one, and implies that some pseudorotaxanes possess more rotaxane-like character than others. Moreover, it shows that the concept of a pseudorotaxane is one that is inherently vague and is best described using fuzzy sets,[14] in which the set of pseudorotaxanes (**P**) belongs (Figure 10), to some extent, to both the set of mechanically interlocked rotaxanes (**R**) and the set of two isolated chemical entities (**I**), i.e., $\mathbf{P} = [\mathbf{R} \cap \mathbf{I}]$, a description that provides much more meaning than one in which a definite cutoff is made between rotaxanes and pseudorotaxanes.

Acknowledgment. This research was sponsored in the U.K. by an Engineering and Physical Sciences Research Council CASE Award (to M.C.T.F.).

Supporting Information Available: Experimental procedures—including the derivation of eq 1—crystallographic data, and ^{1}H NMR spectra (43 pages). See any current masthead page for ordering information and Web access instructions.

JA9731276